



# RNA-binding protein RBM47 stabilizes IFNAR1 mRNA to potentiate host antiviral activity

Kezhen Wang<sup>†</sup> , Chenxiao Huang<sup>†</sup>, Tao Jiang, Zhiqiang Chen, Minfei Xue, Qi Zhang, Jinyu Zhang & Jianfeng Dai<sup>\*†</sup> 

## Abstract

The type I interferon (IFN-I, IFN- $\alpha/\beta$ )-mediated immune response is the first line of host defense against invading viruses. IFN- $\alpha/\beta$  binds to IFN- $\alpha/\beta$  receptors (IFNARs) and triggers the expression of IFN-stimulated genes (ISGs). Thus, stabilization of IFNARs is important for prolonging antiviral activity. Here, we report the induction of an RNA-binding motif-containing protein, RBM47, upon viral infection or interferon stimulation. Using multiple virus infection models, we demonstrate that RBM47 has broad-spectrum antiviral activity *in vitro* and *in vivo*. RBM47 has no noticeable impact on IFN production, but significantly activates the IFN-stimulated response element (ISRE) and enhances the expression of interferon-stimulated genes (ISGs). Mechanistically, RBM47 binds to the 3'UTR of IFNAR1 mRNA, increases mRNA stability, and retards the degradation of IFNAR1. In summary, this study suggests that RBM47 is an interferon-inducible RNA-binding protein that plays an essential role in enhancing host IFN downstream signaling.

**Keywords** IFNAR1; innate immunity; interferon-stimulated genes; RNA-binding protein 47; virus infection

**Subject Categories** Immunology; Microbiology, Virology & Host Pathogen Interaction; RNA Biology

**DOI** 10.15252/embr.202052205 | Received 2 December 2020 | Revised 21 May 2021 | Accepted 25 May 2021 | Published online 23 June 2021

**EMBO Reports (2021) 22: e52205**

## Introduction

The type I interferon (IFN-I, IFN- $\alpha/\beta$ )-mediated innate immune response, considered as the first line of host defense, plays a key role in the clearance of pathogens, especially viruses (Medzhitov & Janeway, 2000). Upon viral infection, IFN- $\alpha/\beta$  is secreted from cells and binds to IFN receptors 1 and 2 (IFNAR1/2) on the cell surface, triggering the Janus kinase signal transducer and activator of transcription (JAK-STAT) pathway through phosphorylation and activation of Janus kinase 1 (JAK1) and tyrosine kinase 2 (TYK2). These kinases subsequently catalyze the recruitment and phosphorylation

of STAT1 and STAT2, leading to translocation of the STAT1-STAT2-IRF9 complex, known as interferon-stimulated gene factor 3 (ISGF3), into the nucleus. This complex then binds to the IFN-stimulated response element (ISRE) within the promoters of IFN-stimulated genes (ISGs) to induce the expression of hundreds of ISGs, which display diverse antiviral effector functions (Sadler & Williams, 2008). Both virus infection and IFN stimulation lead to IFNAR1 phosphorylation, promoting its ubiquitination and accelerating type I IFN signal attenuation (Liu *et al*, 2009; Qian *et al*, 2011; Zheng *et al*, 2011). Defects in IFNAR1 leads to lowered antiviral activity in the host. Hence, stabilization of IFNAR1 is an essential factor in determining and prolonging the antiviral activity in hosts.

Among approximately 20,000 mammalian protein-coding genes, more than 1,500 have been defined as RNA-binding proteins (RBPs). Nearly half of these RBPs are putative mRNA-binding proteins (Gerstberger *et al*, 2014). Some RBPs combine with large ribonucleoproteins (RNPs) to regulate multiple aspects of RNA biogenesis (Chateigner-Boutin & Small, 2011), such as mRNA export, transcript stability, transcript localization, ribosome assembly, RNA splicing, translation, and RNA decay (Kong & Lasko, 2012; Medioni *et al*, 2012; Schoenberg & Maquat, 2012; Bock *et al*, 2015). Individual RBPs may interact with single or multiple RNAs by binding to specific sequences or structures and regulate gene expression at various levels (Turner & Diaz-Munoz, 2018). These functions either occur in the nucleus (He *et al*, 2016), the cytoplasm (Dolezal *et al*, 2017), or within cellular organelles, such as mitochondria (Antonicka & Shoubridge, 2015). By controlling RNA decay and translation, RBPs control gene expression independently of the established transcriptional networks. Recently, RBPs have been found to be essential for the development and function of the immune system. RBPs maintain a poised transcriptome, such as the cytokine mRNAs that are rapidly translated in response to T-cell receptor (TCR) signaling in memory T cells (Hombrink *et al*, 2016; Salerno *et al*, 2017). The roles of RBPs in immunomodulation have led to their emergence as targets for the development of new therapeutic modalities.

Using RNA-seq analysis, we previously identified that an RNA-binding motif protein (RBM), RBM47, is upregulated during dengue virus (DENV) infection (Wang *et al*, 2018). The RBM proteins have been highly conserved in evolution and are capable of binding to RNA with two RNA recognition motif (RRM)

domains. However, the functions of most RBM proteins remain unclear. Like other RBPs, RBM family proteins participate in a variety of RNA processes, including alternative splicing, translation, RNA silencing, and RNA editing, thereby influencing multiple physiological processes (Sutherland *et al*, 2005). For example, RBM3, 5, 6, and 10 are involved in the regulation of apoptosis (Sutherland *et al*, 2005). RBM24 modulates hepatitis B virus replication by targeting the viral RNA (Yao *et al*, 2018). RBM10 exerts a pro-inflammatory function by interacting with the RIG-I receptor activated by the cytoplasmic dengue RNA (Pozzi *et al*, 2020). RBM47 is ubiquitously expressed and plays important roles in post-transcriptional gene regulation by binding to specific mRNAs, mainly in introns and 3'UTRs (Vanharanta *et al*, 2014). RBM47 is a tumor suppressor that inhibits the progression of breast (Vanharanta *et al*, 2014), lung (Sakurai *et al*, 2016), and colon cancers (Rokavec *et al*, 2017) by stabilizing distinct tumor suppressor mRNAs. RBM47 also acts as an alternative splicing factor (Vanharanta *et al*, 2014; Cieply *et al*, 2016; Kim *et al*, 2019), an essential cofactor of APOBEC1-mediated C-to-U RNA editing (Rayon-Estrada *et al*, 2017; Blanc *et al*, 2019), and as a regulator of cell fate decisions (Radine *et al*, 2020). Recently, RBM47 has been shown to elevate IL-10 production by directly binding to the 3'UTR, delaying the degradation of IL-10 mRNA (Wei *et al*, 2019). In this study, we explored the role of RBM47 in viral infections, which was as yet uncharacterized.

## Results

### RBM47 is a novel interferon-stimulated gene

In our previous study using RNA-seq analysis, we found RBM47 in the list of upregulated genes in DENV-infected 293T cells (Wang *et al*, 2018). To confirm this result, we determined the expression of RBM47 in DENV-infected 293T, HFF, HUVEC, and THP-1 cells. As shown in Fig 1A, both the mRNA and protein levels of RBM47 were higher in DENV-infected cells than in non-infected controls. Moreover, Gene Expression Omnibus (GEO) datasets also demonstrated that RBM47 mRNA was upregulated during H5N1 (Lin *et al*, 2015) (Fig EV1A), H1N1 (Gerlach *et al*, 2013) (Fig EV1B), and HCV (Blackham *et al*, 2010; Zhao *et al*, 2013) (Fig EV1C and D) infections. Similarly, RBM47 mRNA and protein levels were elevated in SeV-infected 293T, HFF, HUVEC, and THP-1 cells (Fig 1B), suggesting that RBM47 is a virus-induced gene.

Next, we investigated whether RBM47 is an ISG. The expression of RBM47 in IFN- $\alpha$ -stimulated 293T, HFF, HUVEC, and THP-1 cells was determined using qRT-PCR and Western blot. As shown in Fig 1C, the mRNA and protein levels of RBM47 were significantly upregulated upon IFN- $\alpha$  stimulation. Furthermore, by searching the transcription factor binding elements database JASPAR (<http://jaspar.genereg.net/>), we found that there were three putative STAT1 binding motifs in the RBM47 gene promoter region (Fig 1D), which is critical for IFN induction (Ma *et al*, 2015). The luciferase reporter assay suggested that the promoter of RBM47 (from -2,000 to +100, containing all STAT1 binding motifs) could be activated by SeV infection or IFN- $\alpha$  stimulation (Fig 1E). These results suggest that RBM47 is an ISG that can be induced by viral infection or IFN stimulation.

### RBM47 has broad-spectrum antiviral activity *in vitro*

Since RBM47 is induced by viruses or interferons, we investigated its function in viral infection. We first found that RBM47 restricted the DENV replication because viral RNA and protein levels were significantly lower in RBM47-overexpressing 293T cells than in control cells (Fig 2A). Additionally, a luciferase-based DENV replicon (DGL2) assay (Kato *et al*, 2014; Wang *et al*, 2018) confirmed the antiviral effect of RBM47 on DENV (Fig 2A). To further evaluate the antiviral effect of RBM47, we constructed three shRNA plasmids (sh47-1, sh47-2, and sh47-3) targeting RBM47 mRNA. All the three shRNAs effectively knocked down RBM47 (Fig 2B), and DENV replication was significantly upregulated in RBM47 knockdown cells compared with that in control cells (Fig 2B). Furthermore, RBM47 ectopic expression inhibited replication of Zika virus (ZIKV) (Fig EV2A and B), and knockdown of RBM47 enhanced ZIKV infection (Fig EV2C and D). All these results suggest that RBM47 suppresses these positive single-stranded RNA viruses.

To test whether RBM47 also restricts infection by other viruses, we used two model viruses, VSV and HSV-1, representing negative single-strand RNA and double-stranded DNA viruses, respectively. As shown in Fig 2C, the viral RNA, protein, and progeny levels of VSV were significantly lower in cells ectopically expressing RBM47 than those in control cells. Notably, overexpression of RBM47 also inhibited HSV-1 replication in 293T cells (Fig 2D).

To further confirm these phenotypes, we transfected 293T cells with sh47-3 or control vector (shNC) and then infected the cells with VSV or HSV-1. As shown in Fig 2E and F, cells in which RBM47 was knocked down were more susceptible to VSV and HSV-1 infection, since the viral RNA and proteins significantly increased in RBM47-silenced cells. In addition, the viral titers from the supernatant of RBM47-deficient cells increased significantly (Fig 2E and F) compared to that in the controls. These results demonstrate that RBM47 has broad-spectrum antiviral activity *in vitro*.

### RBM47 enhances the expression of ISGs

Innate immunity is the host's first line of defense against viral invasion. To test whether RBM47 is involved in the regulation of innate antiviral immune responses, such as interferon signaling, and influences IFN production, an IFN- $\beta$ -Luc reporter assay was first performed in 293T cells with or without RBM47 ectopic expression. After stimulation with SeV, we found that the IFN- $\beta$  promoter activity was not significantly influenced by RBM47 (Fig 3A). We then tested whether RBM47 influenced IFN downstream signaling. IFN-responsive ISRE promoter assays were performed, and the results suggested that RBM47 significantly increased ISRE promoter activity after SeV stimulation (Fig 3A). To further confirm the effect of RBM47 on ISRE promoter activation, we used Poly (I: C) or IFN- $\alpha$  to stimulate the cells. As shown in Fig 3B and C, upon Poly (I: C) or IFN- $\alpha$  stimulation, ISRE promoter activity increased in RBM47-overexpressing cells and decreased in RBM47-silenced cells.

We then tested whether RBM47 alters SeV-induced ISG expression and found that the mRNA levels of all the tested ISGs, such as IFIT1, ISG15, and Cig5, increased in RBM47-overexpressing cells

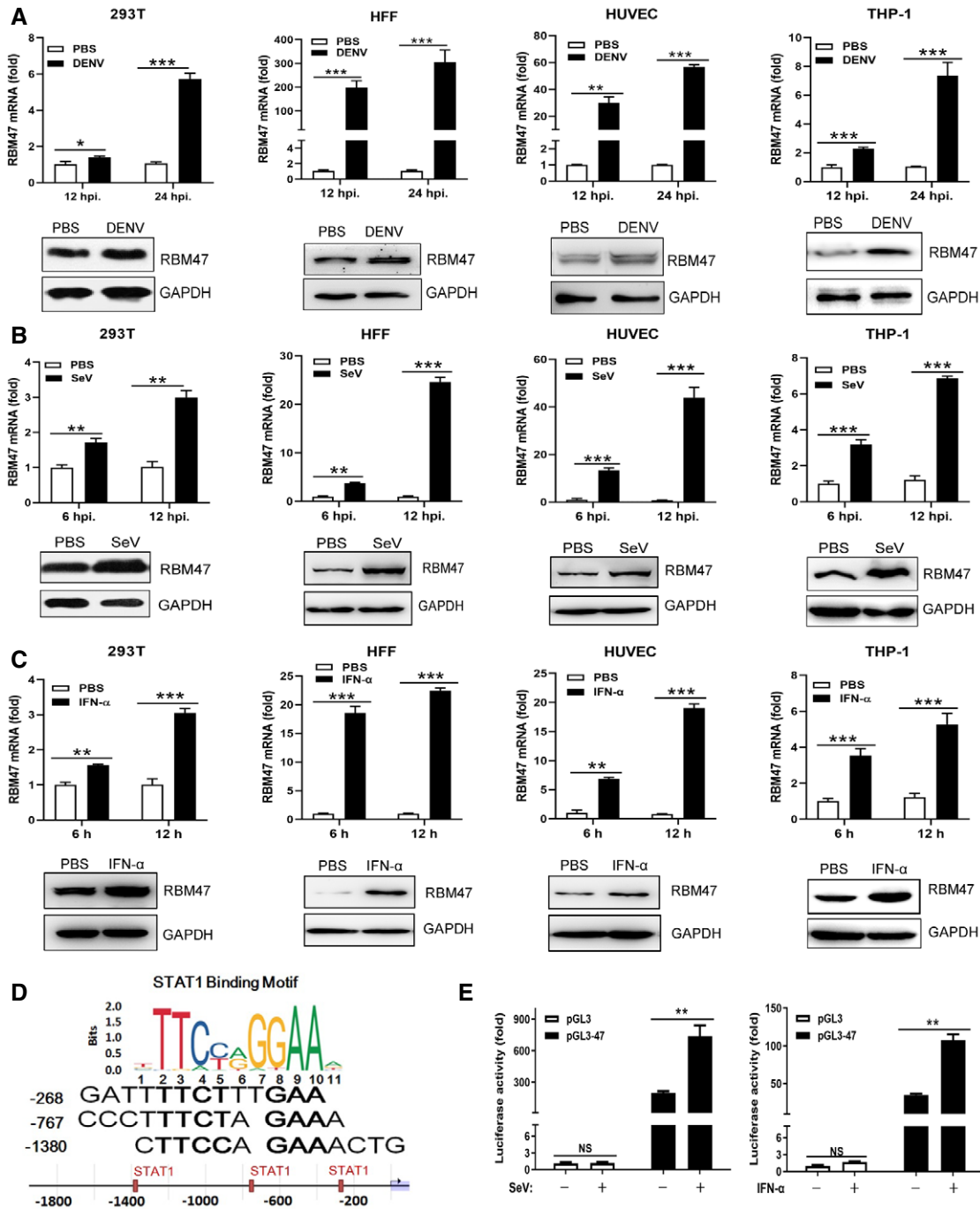


**Figure 1. RBM47 is an interferon-stimulated gene.**

**A** Expression of RBM47 was induced by DENV infection in 293T, HFF, HUVEC, and THP-1 cells. Cells were infected with DENV-2 at an MOI of 1 for 12 or 24 h. The expression of RBM47 mRNA (12- and 24-h post-infection, hpi) and protein (24 hpi) were compared between virus-infected and non-infected cells (PBS). The PCR results are represented as the means  $\pm$  SD of  $n = 3$  biological replicates.

**B, C** Both mRNA and protein levels of RBM47 were elevated in SeV-infected (B) or IFN- $\alpha$ -stimulated (C) 293T, HFF, HUVEC, and THP-1 cells. Cells were infected with SeV (MOI = 1) or stimulated with IFN- $\alpha$  for 6 or 12 h, and the expression of RBM47 mRNA (at 6- and 12-h post-treatment) and protein (at 6- and 12-h post-treatment) was tested. The PCR results are represented as the means  $\pm$  SD of  $n = 3$  biological replicates.

**D** Three putative STAT1 binding motifs in the RBM47 gene promoter region as predicted by using JASPAR (<http://jaspar.genereg.net/>).

**E** The pGL3-RBM47 promoter plasmid (pGL3-47) or the empty vector was transfected into 293T cells, and RBM47 promoter activities were tested upon SeV infection or IFN- $\alpha$  stimulation. Data are represented as the means  $\pm$  SD of  $n = 3$  biological replicates.

Data information: Data in A-C and E are representative of  $n = 3$  independent experiments. NS, non-significant; \* $P \leq 0.05$ , \*\* $P \leq 0.01$ , and \*\*\* $P \leq 0.001$  (Student's  $t$ -test). Source data are available online for this figure.

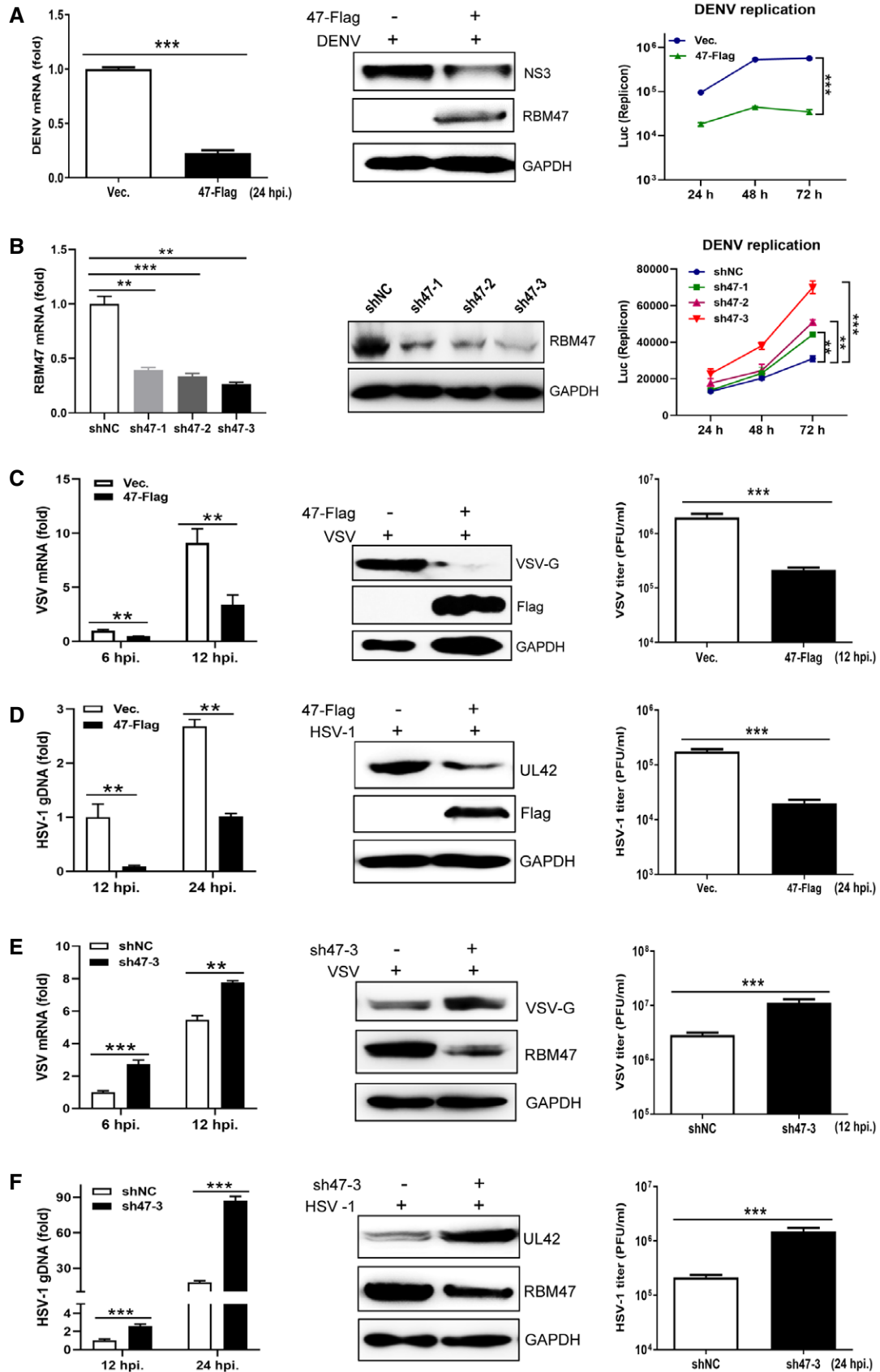


Figure 2.

**Figure 2. RBM47 displays antiviral activity.**

A The mRNA and protein levels of DENV (left and middle panel) and DENV replicon DGL2 replication (right panel) were tested in 293T cells transfected with RBM47-Flag or empty vector at the indicated time points. The PCR and the luciferase data are represented as the means  $\pm$  SD of  $n = 3$  biological replicates.  
 B Knockdown efficiency of three shRNAs against RBM47 was measured using RT-PCR (left panel) and Western blot (middle panel). DENV replicon DGL2 replication was tested in 293T cells transfected with scramble shRNA (shNC) or RBM47 shRNAs (right panel). The PCR and the luciferase data are represented as the means  $\pm$  SD of  $n = 3$  biological replicates.  
 C, D Levels of viral genome, protein, and progeny of VSV (C) or HSV-1 (D) were quantified in virus-infected 293T cells with or without RBM47 ectopic expression at the indicated time points. The viral protein levels were tested 12-h post-VSV infection and 24-h post-HSV-1 infection. The PCR and viral titer data are represented as the means  $\pm$  SD of  $n = 3$  biological replicates.  
 E, F Levels of viral genome, protein, and progeny of VSV (E) or HSV-1 (F) from virus-infected 293T cells transfected with RBM47 shRNA or shNC at the indicated time points. The PCR and viral titer data are represented as the means  $\pm$  SD of  $n = 3$  biological replicates.  
 Data information: The data shown are representative of  $n = 3$  independent experiments.  $**P \leq 0.01$ , and  $***P \leq 0.001$  (Student's *t*-test).  
 Source data are available online for this figure.

compared with that in controls (Fig 3D). In line with this, the mRNA levels of IFIT1, ISG15, and Cig5 decreased significantly in cells in which RBM47 was knocked down (Fig 3E).

Consistent with the above results, IFN- $\alpha$ -induced expression of ISGs was upregulated in 293T cells ectopically expressing RBM47 (Fig 3F) and downregulated in RBM47-silenced mouse peritoneal macrophages (PMs) compared with that in the controls (Fig 3G). These results demonstrate that RBM47 does not influence the production of type one IFN, but enhances the expression of ISGs.

**RBM47 modulates IFNAR1 mRNA stability**

Since RBM47 amplifies the expression of ISGs in virus-infected or IFN-stimulated cells, we investigated the mode of action of RBM47 in JAK-STAT signaling pathway. We first identified the RNAs that bind to RBM47 using an RNA immunoprecipitation (RIP) assay (Fig EV3A). Among the RBM47-bound RNAs, we found that the mRNAs of IFNAR1 and IFNAR2 provided two potential targets of RBM47 (Fig EV3B). We further confirmed the results of RIP assays using qRT-PCR. This showed that only IFNAR1 mRNA was

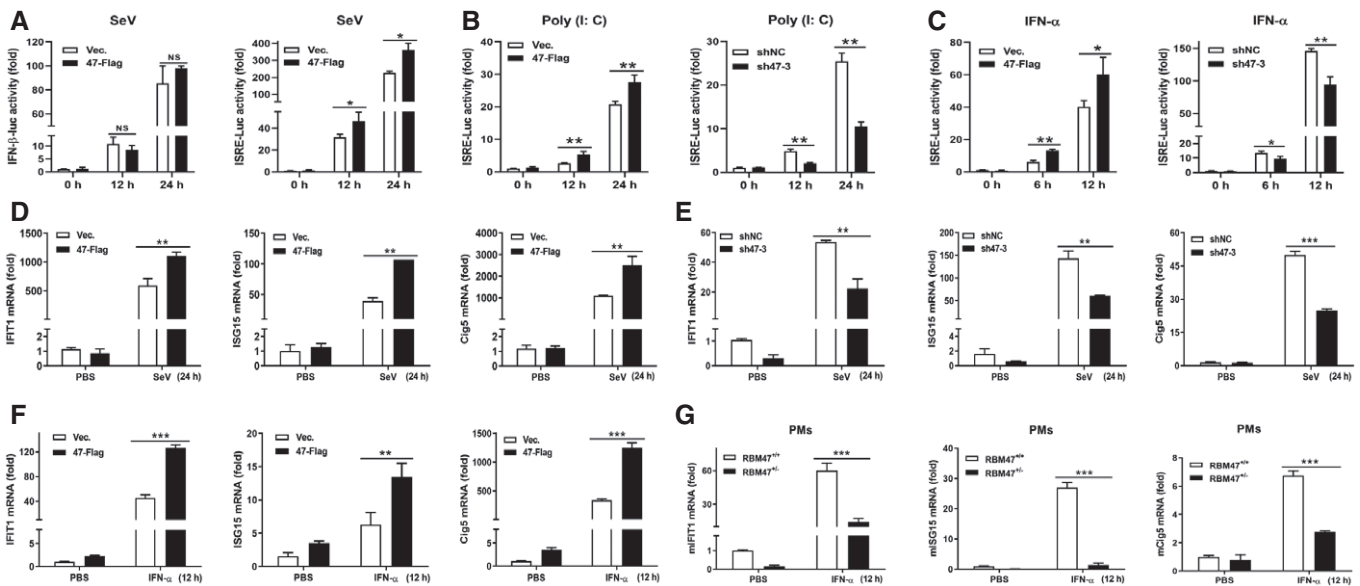


**Figure 3. RBM47 enhances the expression of ISGs.**

A Promoter activity of IFN- $\beta$  or ISRE in SeV-infected 293T cells with or without RBM47 ectopic expression. Cells were infected with SeV for 12 and 24 h, and the promoter activities were determined using the DLR assay. Data are represented as the means  $\pm$  SD of  $n = 3$  biological replicates.  
 B, C Promoter activities of ISRE stimulated by Poly (I: C) (B) or IFN- $\alpha$  (C) in RBM47-overexpressing or knockdown 293T cells. Cells were stimulated with Poly (I: C) (1  $\mu$ g/ml) or IFN- $\alpha$  (200 U/ml) for the indicated time, and the ISRE promoter activities were determined using the DLR assay. Data are represented as the means  $\pm$  SD of  $n = 3$  biological replicates.  
 D, E mRNA expression of IFIT1, ISG15, and Cig5 in SeV-infected 293T cells overexpressing RBM47 (D) or RBM47 knocked down cells (E). Cells were infected with SeV for 24 h, and gene expression was determined using qRT-PCR. The PCR results are represented as the means  $\pm$  SD of  $n = 3$  biological replicates.  
 F The expression of IFIT1, ISG15, and Cig5 in RBM47-overexpressing or control 293T cells stimulated by IFN- $\alpha$  for 12 h. The PCR results are represented as the means  $\pm$  SD of  $n = 3$  biological replicates.  
 G The expression of IFIT1, ISG15, and Cig5 in WT and RBM47 $^{-/-}$  peritoneal macrophages stimulated by IFN- $\alpha$  for 12 h. The PCR results are represented as the means  $\pm$  SD of  $n = 3$  biological replicates.  
 Data information: The data shown are representative of  $n = 3$  independent experiments. NS, non-significant;  $*P \leq 0.05$ ,  $**P \leq 0.01$ , and  $***P \leq 0.001$  (Student's *t*-test).

significantly enriched by RBM47-Flag immunoprecipitation (Fig 4A), which was consistent with the data from a genome-wide HITS-CLIP (POSTAR2, <http://lulab.life.tsinghua.edu.cn/postar/index.php>). Therefore, we speculated that the identification of IFNAR2 mRNA in RIP-Seq assays might be due to indirect interactions between RNA-binding proteins and RNAs.

To test the effect of RBM47 on IFNAR1 mRNA stabilization, we transfected 293T cells with RBM47-Flag or empty vector for 24 h and then treated the cells with 5, 6-dichloro-1- $\beta$ -D-ribofuranosylbenzimidazole (DRB), an inhibitor of RNA synthesis. Cells were harvested at 0, 15, 30, 45, and 60 min after DRB treatment, and the total RNA was subjected to qRT-PCR analysis.

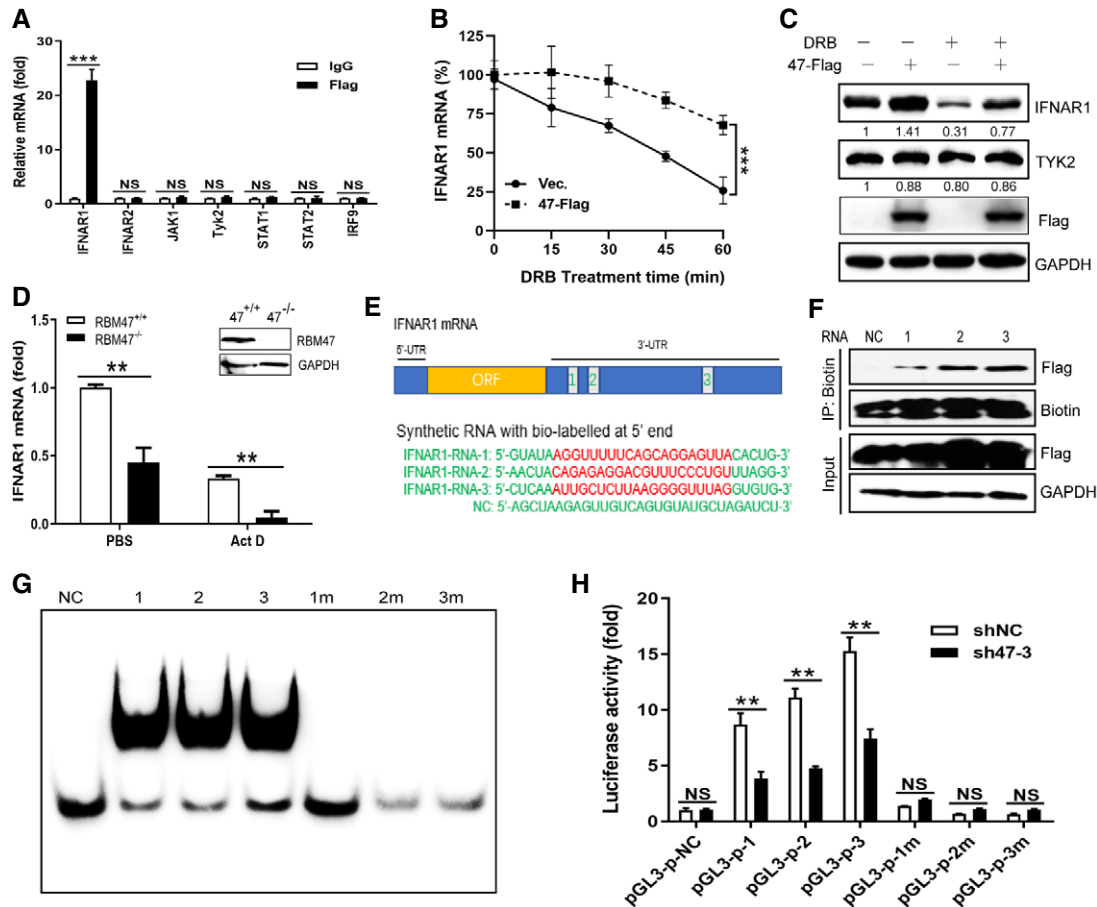


**Figure 4. IFNAR1 mRNA is stabilized by RBM47.**

- A Relative mRNA levels of JAK-STAT signaling adaptors were determined using RIP-PCR analysis. The enrichment folds of each gene relative to the IgG isotype group (which was set to "1") are shown. The PCR results are represented as the means  $\pm$  SD of  $n = 3$  biological replicates.
- B IFNAR1 mRNA stability after DRB treatment. 293T cells were transfected with RBM47-Flag or empty vectors and treated with DRB (50  $\mu$ g/ml). Total RNA was harvested at 0, 15, 30, 45, and 60 min, and IFNAR1 mRNA levels were measured using qRT-PCR and normalized to  $\beta$ -actin. The PCR results are represented as the means  $\pm$  SD of  $n = 3$  biological replicates.
- C The protein levels of IFNAR1 and TYK2 in RBM47-overexpressing or control 293T cells treated with or without DRB. The relative band density was quantified using the ImageJ software and normalized to GAPDH. The relative density of the control group was set to "1."
- D IFNAR1 mRNA expression in WT and RBM47 knockout 293T cells treated with or without RNA synthesis inhibitor Act D. The knockout efficiency of RBM47 is shown in the upper-right panel. The PCR results are represented as the means  $\pm$  SD of  $n = 3$  biological replicates.
- E Locations and sequences of three RBM47-targeted RNA sequences at the 3'UTR of IFNAR1 mRNA. Data were obtained from a genome-wide HITS-CLIP database (POSTAR2, <http://lulab.life.tsinghua.edu.cn/postar/index.php>). The predicted RBM47-binding sequences were labeled in red.
- F RNA pull-down assays using biotin-labeled RNA probes. The cell lysates with RBM47-flag were immunoprecipitated with biotin-conjugated RNA probes, and the elution was blotted with an anti-Flag antibody.
- G Interaction between RBM47 and the three RNA fragments of IFNAR1 mRNA confirmed using EMSA assay. RBM47 binds to IFNAR1 RNA probes but not to mutant (1m, 2m, and 3m) or negative control (NC) probes.
- H The interaction between RBM47 and the three targeted RNA fragments from the 3'UTR of IFNAR1 mRNA was tested using the luciferase reporter assay. The U to A mutants of these three sequences (as shown in Table EV1) were also used as negative controls. Data are represented as the means  $\pm$  SD of  $n = 3$  biological replicates.

Data information: Data in A-D and F-H are representative of  $n = 3$  independent experiments. NS, non-significant;  $**P \leq 0.01$ , and  $***P \leq 0.001$  (Student's *t*-test). Source data are available online for this figure.

The results revealed that overexpression of RBM47 delayed the degradation of IFNAR1 mRNA (Fig 4B). Subsequently, we also found increased IFNAR1 protein levels in the presence of RBM47 overexpression, with or without DRB treatment (Fig 4C). To further confirm this result, we generated an RBM47 knockout cell line and treated the cells with actinomycin D (Act D), another RNA synthesis blocker. As shown in Fig 4D, before Act D treatment, the amount of IFNAR1 mRNA was significantly lower in RBM47 knockout cells than in controls. After Act D treatment, IFNAR1 mRNA degraded faster in RBM47 knockout cells than in control cells.

Using sequences from genome-wide HITS-CLIP, three biotin-labeled RNA probes from the 3'UTR of IFNAR1 mRNA were

synthesized for RNA pull-down assays using RBM47 (Fig 4E). As shown in Fig 4F, RBM47 was pulled out by all three biotin-labeled RNA probes, but not by the negative control RNA probe. The electrophoretic mobility shift assay (EMSA) also confirmed the interaction between RBM47 and the three RNA fragments of IFNAR1 mRNA (Fig 4G). Simultaneously, these three RNA fragments and their matching mutants were individually inserted into a pGL3 promoter vector at the end of luciferase open reading frame (ORF). The luciferase reporter assays showed that all three IFNAR1-related RNA fragments, rather than their mutants, enhanced luciferase expression (Fig 4H). In line with our prediction, luciferase expression significantly reduced in the shRBM47 group compared to that in the shNC group (Fig 4H).

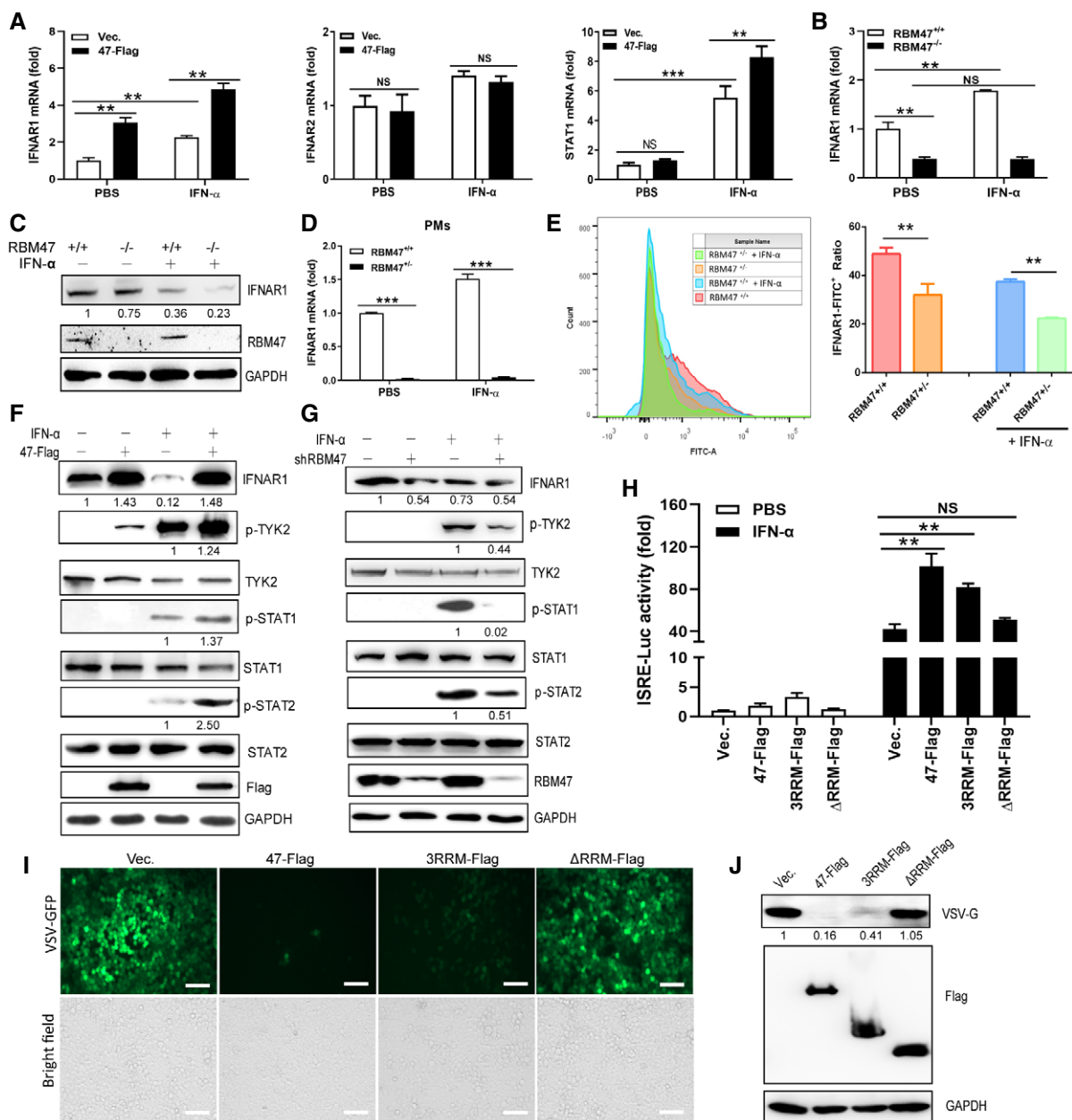


Figure 5.

**Figure 5. RBM47 enhances the JAK-STAT pathway.**

- A mRNA of IFNAR1, but not IFNAR2 or STAT1, was stabilized by RBM47 ectopic expression in 293T cells with or without IFN- $\alpha$  stimulation. Cells were treated with IFN- $\alpha$  or PBS for 6 h, and the relative gene expression levels were determined using qRT-PCR. The PCR results are represented as the means  $\pm$  SD of  $n = 3$  biological replicates.
- B, C mRNA (B) and protein (C) levels of IFNAR1 were analyzed in WT and RBM47 knockout 293T cells with or without IFN- $\alpha$  stimulation. The relative density of IFNAR1 protein in the control group was set to "1". The PCR results are represented as the means  $\pm$  SD of  $n = 3$  biological replicates.
- D IFNAR1 mRNA expression in PMs from WT and RBM47<sup>+/-</sup> mice treated with or without IFN- $\alpha$ . The PCR results are represented as the means  $\pm$  SD of  $n = 3$  biological replicates.
- E Flow cytometry analysis of IFNAR1 in the cytoplasmic membrane of BMDMs from WT and RBM47<sup>+/-</sup> mice. The cells were treated with PBS or IFN- $\alpha$  for 6 h. Data are represented as the means  $\pm$  SD of  $n = 3$  biological replicates.
- F, G Protein levels of IFNAR1 and phosphorylation levels of TYK2, STAT1, and STAT2 in RBM47-overexpressing (F) or knockdown (G) 293T cells. Cells were treated with PBS or IFN- $\alpha$  for 6 h, and the relative band densities were analyzed using ImageJ software and normalized to GAPDH.
- H ISRE luciferase was tested to investigate the effects of RBM47 or its variants on ISG activation stimulated by IFN- $\alpha$ . Data are represented as the means  $\pm$  SD of  $n = 3$  biological replicates.
- I, J Effect of overexpression of WT or RBM47 mutants on VSV replication. 293T cells were transfected with RBM47-Flag or two mutants for 24 h and then infected with GFP-expressing VSV (MOI = 0.1) for another 12 h. The replication of VSV was observed using fluorescence microscopy via GFP signal (I) (Scale bar, 50  $\mu$ m), and protein levels were determined using Western blot (J). The relative band densities were analyzed using ImageJ software and normalized to GAPDH. The relative density of VSVG protein in the control group was set to "1".

Data information: The data shown are representative of  $n = 3$  independent experiments. NS, non-significant; \*\* $P \leq 0.01$ , and \*\*\* $P \leq 0.001$  (Student's *t*-test). The data shown are representative of three independent experiments. Source data are available online for this figure.

**RBM47 amplifies the JAK-STAT pathway**

We further tested the effect of RBM47 on IFNAR1 expression following IFN- $\alpha$  stimulation. As shown in Fig 5A, mRNA of IFNAR1, rather than IFNAR2, was stabilized by RBM47 in IFN- $\alpha$ -stimulated 293T cells. RBM47 did not stabilize STAT1, which was used as a control. To further confirm the effect of RBM47 on IFNAR1 mRNA, the RBM47 knockout cell line was stimulated with IFN- $\alpha$ . RT-PCR assays showed that the content of IFNAR1 mRNA in RBM47 knockout cells was less than that in wild-type cells, regardless of IFN- $\alpha$  stimulation (Fig 5B). Western blot analysis also demonstrated that IFNAR1 protein levels were lower in RBM47 knockout cells than in wild-type cells (Fig 5C).

To further confirm the action of RBM47 on the expression of ISGs, we determined the expression of IFNAR1 in macrophages isolated from wild-type and RBM47 heterozygous mice. As shown in Fig 5D, the IFNAR1 mRNA was severely depleted in PMs from RBM47 heterozygous mice compared with that in PMs from WT mice. Furthermore, endogenous IFNAR1 levels on the

cytoplasmic membrane of mouse bone marrow-derived macrophages (BMDMs) were evidently reduced in RBM47 heterozygous mice (Fig 5E).

Since RBM47 stabilized the IFNAR1 mRNA, the effect of RBM47 on the JAK-STAT pathway was investigated. 293T cells were first transfected with RBM47-Flag or empty vector and then treated with IFN- $\alpha$ . The results showed that the protein level of IFNAR1 was enhanced by RBM47 overexpression in cells regardless of IFN- $\alpha$  stimulation (Fig 5F). Meanwhile, the phosphorylation levels of TYK2, STAT1, and STAT2 also increased significantly with ectopic expression of RBM47 (Fig 5F). Similarly, IFNAR1 expression and the phosphorylation levels of TYK2, STAT1, and STAT2 were reduced significantly in RBM47 knocked down cells (Fig 5G).

In accordance with a previous study (Fossat *et al*, 2014), we generated two RBM47 mutant isoforms: the 3RRM variant form that had the three RNA recognition motifs (RRM) and the  $\Delta$ RRM variant that lacked the RRM. The reporter assay suggested that both full-length RBM47 and the 3RRM variant, rather than the

**Figure 6. RBM47 displays antiviral activity *in vivo*.**

- A Immunoblot analysis of RBM47 and IFNAR1 in the lungs, livers, and spleens of RBM47<sup>+/+</sup> (WT) and RBM47<sup>+/-</sup> mice. Each band represents tissue samples from one mouse.
- B Analysis of viral mRNA from blood, lung, brain, and spleen samples of RBM47<sup>+/+</sup> and RBM47<sup>+/-</sup> mice ( $n = 6$  per group) infected with VSV ( $1 \times 10^8$  pfu), and the results were normalized to those of mouse  $\beta$ -actin. Each dot represents data from one mouse. The PCR results are represented as the means  $\pm$  SD of  $n = 6$  biological replicates.
- C Viral titers in serum, lung, brain, and spleen samples of RBM47<sup>+/+</sup> and RBM47<sup>+/-</sup> mice at day 1 post-VSV infection. The viral titer data are represented as the means  $\pm$  SD of  $n = 6$  biological replicates.
- D Micrographs of hematoxylin-and-eosin-stained lung sections from mice treated with PBS or VSV (day-1 post-infection). Scale bar, 50  $\mu$ m.
- E IFN- $\beta$  protein levels in the serum of RBM47<sup>+/+</sup> and RBM47<sup>+/-</sup> mice determined using IFN- $\beta$  ELISA kit. Data are represented as the means  $\pm$  SD of  $n = 6$  biological replicates.
- F qPCR analysis of IFNAR1, IFIT1, and Cig5 mRNA in the blood samples of infected mice. The relative expression levels of genes in WT mice were set to "1". The PCR results are represented as the means  $\pm$  SD of  $n = 6$  biological replicates.
- G RBM47<sup>+/+</sup> and RBM47<sup>+/-</sup> mice were infected with HSV-1 ( $1 \times 10^7$  pfu) via caudal vein injection. Viral genome DNA and progeny titers were tested using blood samples from infected mice. Data are represented as the means  $\pm$  SD of  $n = 6$  biological replicates.
- H qRT-PCR analysis of IFNAR1 and Cig5 mRNA in blood samples from HSV-1-infected mice. The PCR results are represented as the means  $\pm$  SD of  $n = 6$  biological replicates.

Data information: The data shown are representative of  $n = 3$  independent experiments. NS, non-significant; \* $P \leq 0.05$ , \*\* $P \leq 0.01$ , and \*\*\* $P \leq 0.001$  (Student's *t*-test). Source data are available online for this figure.



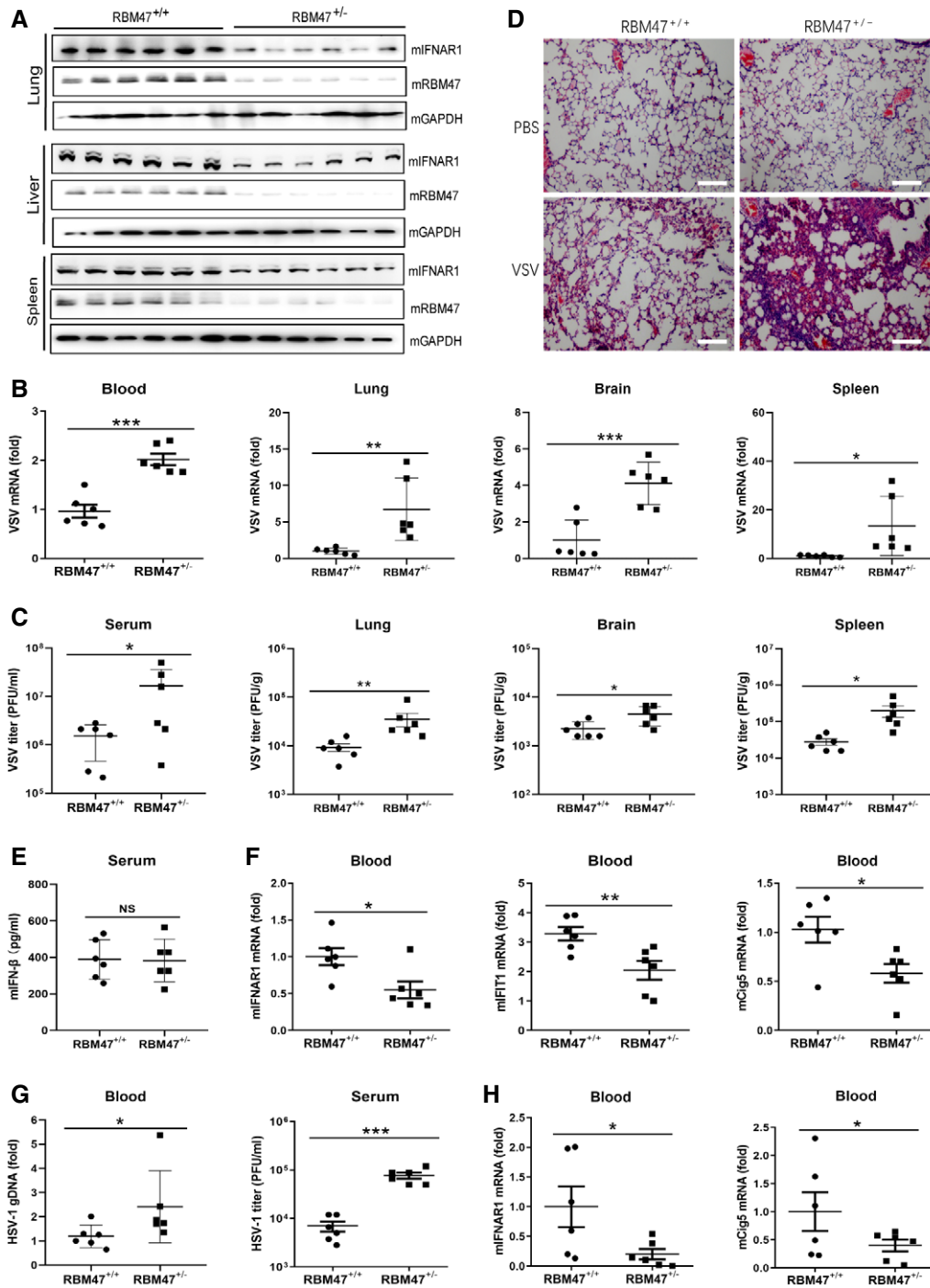


Figure 6.

ΔRRM mutant, enhanced the promoter activity of ISRE induced by IFN-α (Fig 5H). Fluorescence microscopy results showed that the replication of VSV-GFP, as represented by the green fluorescent protein (GFP) signal, substantially decreased in both RBM47- and 3RRM-variant overexpressing 293T cells, but not in ΔRRM mutant ectopically expressed cells (Fig 5I). Western blot results also confirmed this finding (Fig 5J). These data indicate that the RNA recognition domain of RBM47 is essential for its antiviral function.

### RBM47 has antiviral activity *in vivo*

To further confirm the antiviral activity of RBM47 *in vivo*, we generated RBM47 knockout mice. However, we did not obtain RBM47<sup>-/-</sup> homozygous mice, which is consistent with the results of a previous report (Fossat *et al*, 2014). Even so, the protein levels of RBM47, as well as IFNAR1, were significantly lower in multiple tissues of RBM47 heterozygous mice than in those of WT mice (Fig 6A). We then challenged RBM47<sup>+/-</sup> and WT mice with viruses. As shown in

Fig 6B, we found that the viral mRNA levels in the blood, lung, spleen, and brain were significantly higher in the blood samples from VSV-infected RBM47<sup>+/-</sup> mice than in those of WT control mice. The viral titers in these samples from VSV-infected RBM47<sup>+/-</sup> mice were also higher than in those from WT controls (Fig 6C). Histological analysis further indicated that there was more severe tissue injury in the lungs of VSV-infected RBM47<sup>+/-</sup> mice than in those of WT mice (Fig 6D). Furthermore, we found that the expression of IFN- $\beta$  was not influenced (Fig 6E), but the mRNA levels of IFNAR1, IFIT1, and Cig5 were significantly lower in the blood cells of RBM47<sup>+/-</sup> mice (Fig 6F). However, the expression of IFN- $\beta$  (Fig EV4A), IL-6 (Fig EV4B), and TNF- $\alpha$  (Fig EV4C) in the brain and spleen from VSV-infected RBM47<sup>+/-</sup> and WT mice did not differ greatly.

We also infected WT and RBM47<sup>+/-</sup> mice with HSV-1. The copy number of viral genomic DNA and viral titers were significantly higher in the blood samples from RBM47<sup>+/-</sup> mice than in those from WT controls (Fig 6G). Moreover, the mRNA levels of IFNAR1 and Cig5 were also decreased in the blood cells of RBM47<sup>+/-</sup> mice compared with that in those of the controls (Fig 6H). These results demonstrate that RBM47 also modulates IFNAR1 mRNA stability and displays antiviral activity *in vivo*.

### The antiviral effect of RBM47 is IFNAR1 dependent

To investigate whether the antiviral effect of RBM47 relies on its binding to IFNAR1 mRNA, we isolated mouse embryonic fibroblast (MEF) cells from WT and IFNAR1<sup>-/-</sup> mice to test the antiviral capacity of RBM47. First, we observed that the expression of RBM47 was induced in IFNAR1<sup>+/-</sup> cells upon SeV or IFN stimulation, but this induction was disappeared in IFNAR1<sup>-/-</sup> cells (Fig 7A). This result further suggested that RBM47 is an ISG and its induction depends on IFNAR1 signaling.

We then successfully silenced RBM47 in both IFNAR1<sup>+/-</sup> and IFNAR1<sup>-/-</sup> MEFs by shRNA lentivirus against mouse RBM47 (Fig 7B). In wild-type MEFs, after infection with VSV or HSV-1, viral replication increased in the RBM47 knockdown group compared with that in the shNC controls (Fig 7C). However, the replication of both viruses was not significantly influenced in IFNAR1-deficient cells when RBM47 was knocked down (Fig 7C).

To further confirm this phenotype, we treated IFNAR1-deficient (IFNAR1<sup>-/-</sup>) mice with shRBM47 or negative control lentiviruses via caudal vein injection. Seven-day post-lentivirus infection, mice were challenged with VSV by intranasal drip. The mRNA level of RBM47 decreased in shRBM47-treated mice, suggesting that RBM47 was successfully knocked down in these mice (Fig 7D). However, the replication of VSV was not influenced in RBM47 knockdown IFNAR1<sup>-/-</sup> mice compared to that in the normal group (Fig 7D). These results demonstrate that the antiviral activity of RBM47 depends on its capacity to stabilize IFNAR1 mRNA.

From these data, we speculated that RBM47 is induced upon virus infection and enhances host antiviral responses by stabilizing IFNAR1 mRNA (Fig 8).

## Discussion

By interacting with RNA and other regulatory molecules, RBPs are functionally integrated into signal transduction, metabolic, and

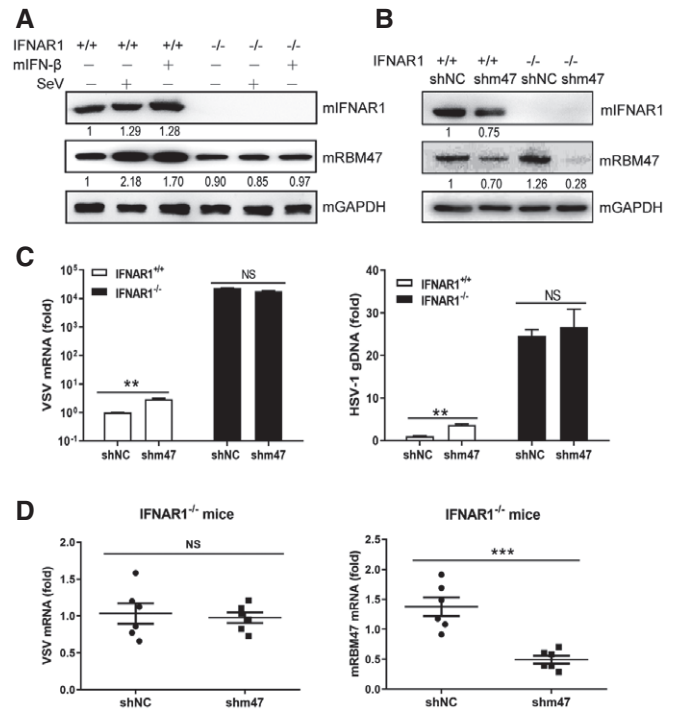


**Figure 7. The antiviral activity of RBM47 is IFNAR1 dependent.**

- A IFNAR1<sup>+/-</sup> and IFNAR1<sup>-/-</sup> MEF cells were stimulated with IFN- $\beta$  or infected with SeV, and the expression of IFNAR1 and RBM47 was determined using Western blot. The gray values of the blots were analyzed using ImageJ software and normalized to GAPDH. The relative density of the control group was set to "1".
- B IFNAR1<sup>+/-</sup> and IFNAR1<sup>-/-</sup> MEFs were infected with shRBM47 or control lentivirus, and the knockdown efficiency of RBM47 was determined using western blot. The relative band densities were analyzed using ImageJ software and normalized to GAPDH.
- C RBM47-deficient or control IFNAR1<sup>+/-</sup> and IFNAR1<sup>-/-</sup> MEFs were infected with VSV or HSV-1. The cells were harvested at 12 hpi. (VSV) or 24 hpi. (HSV-1), and viral RNA levels were analyzed using qRT-PCR. The PCR results are represented as the means  $\pm$  SD of  $n = 3$  biological replicates.
- D The mRNA levels of VSV and RBM47 in blood samples of IFNAR1-deficient (IFNAR1<sup>-/-</sup>) mice ( $n = 6$  per group) infected with VSV. Mice were infected with shRBM47 or control lentivirus for 7 days and then challenged with VSV for another 24 h. Each dot represents one mouse. The PCR results are represented as the means  $\pm$  SD of  $n = 6$  biological replicates.

Data information: The data shown are representative of  $n = 3$  independent experiments. NS, non-significant; \*\* $P \leq 0.01$ , and \*\*\* $P \leq 0.001$  (Student's *t*-test).

Source data are available online for this figure.

transcriptional networks. Although increasing evidence suggests that RBPs may regulate immune responses, the functions of RBPs in antiviral immune regulation remain unclear. In this study, we found that RBM47 is a novel IFN-dependent ISG, which is upregulated in virus-infected or IFN-stimulated cells and has a broad-spectrum antiviral activity *in vitro* and *in vivo*. Recently, another RBM protein, RBM10, was reported to have anti-DENV activity (Pozzi *et al*, 2020). Our unpublished data suggest that other RBM family members, such as RBM3, RBM11, and RBM15 are upregulated during DENV or ZIKV infection. These results suggest that an increasing number of RBM proteins may be involved in virus–host interactions.

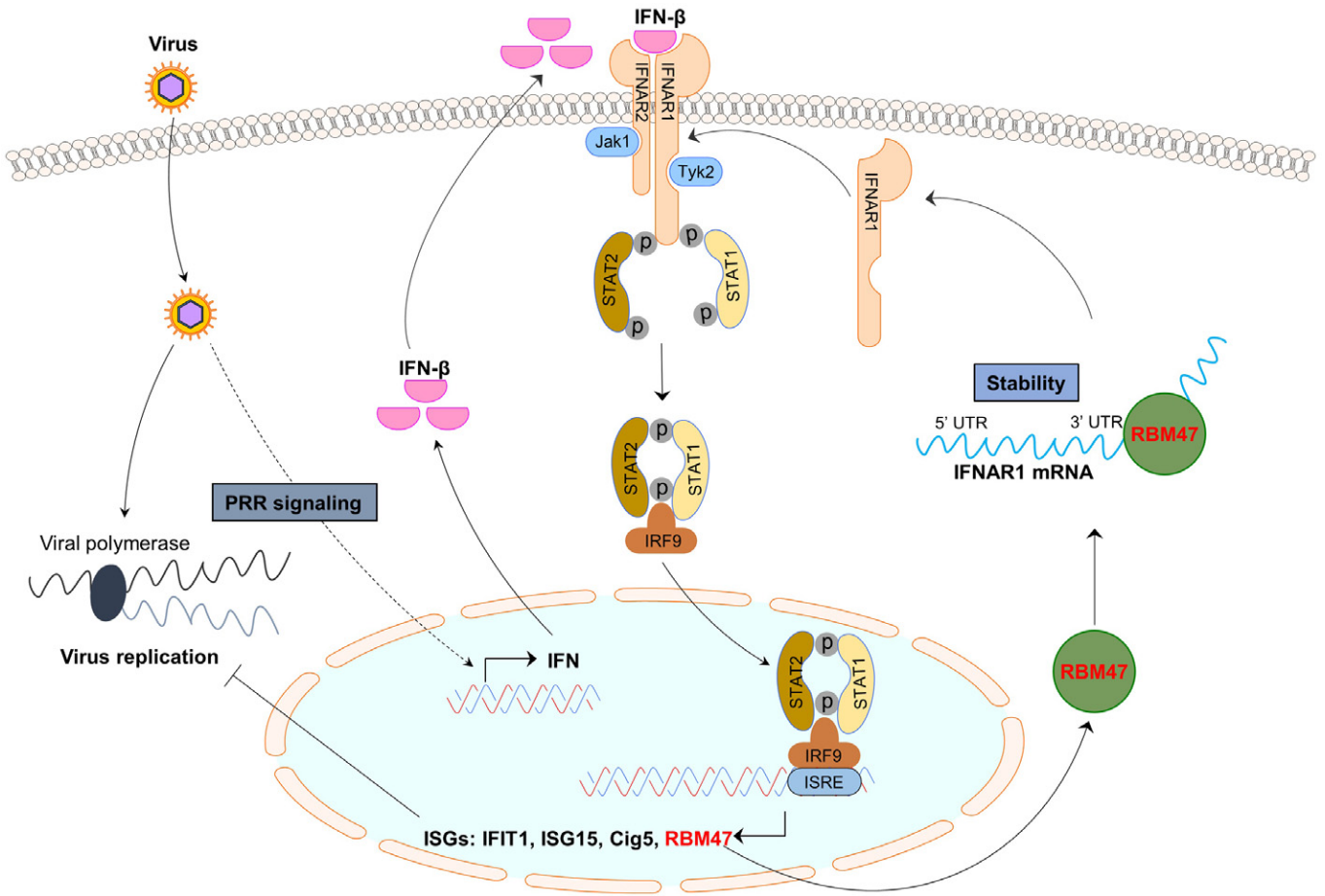


**Figure 8. Model for regulation of IFNAR1 signaling by RBM47.**

RBM47 is an ISG and induced by viral infection. RBM47 binds to the 3'UTR of IFNAR1 mRNA, stabilizes it, and amplifies IFNAR1 signaling.

Since RBM proteins have multiple roles in RNA processing, the antiviral mechanisms of RBM47 may be complicated. Pozzi *et al* (2020) reported that RBM10 may restrict DENV replication by interacting with RIG-I or splicing the mRNA of the antiviral protein spermidine/spermine-N1-acetyltransferase (SAT1). In this study, we found that RBM47 binds to IFNAR1 mRNA, which helps stabilize IFNAR1 mRNA and amplify IFNAR1 signaling. Our experiments using IFNAR1<sup>-/-</sup> cells further confirmed that the antiviral activity of RBM47 relies on IFNAR1 expression. These results suggest that different RBM proteins may target their own protein partners or distinct RNA substrates to perform their functions.

RBM47 may participate in developmental processes (Guan *et al*, 2013); therefore, most homozygous RBM47 knockout mice die within 10–11 days of gestation, and the few surviving RBM47<sup>-/-</sup> mice were significantly smaller than their wild-type counterparts (Fossat *et al*, 2016). Thus, we could not derive RBM47<sup>-/-</sup> mice from the breeding pairs of RBM47<sup>+/-</sup> mice. We found that the expression of RBM47 was significantly downregulated in RBM heterozygous mice. Upon viral infection, the expression of ISGs in RBM47<sup>+/-</sup> mice was significantly lower, and the viral loads increased dramatically. These results suggest that sufficient expression of RBM47 is required for the control of viral infection *in vivo*.

Notably, a recent study reported that zebrafish RBM47 could bind to MAVS and suppress IFN production (Lu *et al*, 2020). However, in our mammalian models, we found that human or mouse RBM47 did not influence IFN production but amplified IFN downstream signaling by binding to IFNAR1 mRNA. Our findings are consistent with the findings of Vanharanta *et al* (2014) who reported that in MDA231 human breast cancer cells, overexpressing RBM47 resulted in obvious upregulation of various ISGs such as ISG15, OAS1, and IRF7. Several studies have defined RBM47 as a tumor suppressor in multiple human cancers (Vanharanta *et al*, 2014; Radine *et al*, 2020). We speculate that promoting IFNAR1 signaling may contribute to the anti-tumor activity of RBM47.

Lipopolysaccharides (LPS) and TNF induce systemic inflammatory response syndrome (SIRS), which involves a strong induction of ISGs (Van Looveren *et al*, 2020) and the degradation of the IFNAR1 protein serves to protect tissues from excessive damage (Bhattacharya *et al*, 2014). Since RBM47 presumably stabilizes IFNAR1, whether RBM47 can act as a potential target for treating inflammatory diseases needs to be further investigated. On the other hand, RBM47 also stabilizes the mRNA of IL-10 (Wei *et al*, 2019), an immunosuppressive cytokine, in specific cells. The detailed role of RBM47 in different cells in inflammation models should be

addressed carefully. Altogether, our study demonstrated that RBM47 binds to IFNAR1 mRNA and amplifies host antiviral activity. This finding provides new evidence that distinct RBPs play critical roles in antiviral immunity.

## Materials and Methods

### Cells, virus, and mice

293T, Vero, HUVEC, HFF, THP-1, and HeLa cells were obtained from ATCC (Manassas, USA) and cultured in Dulbecco's modified Eagle's medium (DMEM) supplemented with 10% FBS and antibiotics/antimycotics.

The DENV type 2 New Guinea C (NGC) strain and ZIKV MR766 strain were propagated in mosquito C6/36 cells (ATCC). The VSV-green fluorescent protein (GFP) virus, which expresses GFP as a non-structural protein, was provided by Dr. Chunsheng Dong (Soochow University). Both VSV-GFP virus and human herpesvirus 1 (HSV-1) were propagated in Vero cells. Cells were infected with viruses at a multiplicity of infection (MOI) of 1, unless otherwise stated.

C57BL/6J mice were obtained from the Shanghai Laboratory Animal Center (Shanghai, China). IFNAR1<sup>-/-</sup> mice (C57BL/6J background) were obtained from the Institute of Medical Laboratory Animal Research, Chinese Academy of Medical Sciences (Beijing, China). RBM47 heterozygous mice were obtained from the CAM-SU Genomic Resource Center of Soochow University. All animals were maintained in biosafety level 2 animal facilities, and experiments were conducted according to the Guide for the Care and Use of Medical Laboratory Animals (Ministry of Health, People's Republic of China) and approved by the Animal Care and Use Committee of Soochow University.

### Antibodies and reagents

The following antibodies were used in this study: mouse anti-GAPDH (Proteintech, Cat # 60004-I-Ig), mouse anti-Flag (ABclonal, Cat # AE005), anti-rabbit IgG HRP-linked antibody (CST, Cat # 7074), rabbit anti-Myc (Proteintech, Cat # I6286-I-AP), rabbit anti-STAT2 (CST, Cat # 72604S), mouse anti-VSV-G (Abgent, Cat # AP1016a), rabbit anti-p-STAT2 (CST, Cat # 88410S), rabbit anti-RBM47 (Abcam, Cat # ab167164), rabbit anti-STAT1 (ABclonal, Cat # A12075), rabbit anti-p-STAT1 (CST, Cat # 9167S), rabbit anti-JAK1 (SAB, Cat # 21119), rabbit anti-IRF9 (Affinity, Cat # DF8179), rabbit anti-Biotin (Abcam, Cat # ab53494), rabbit anti-TYK2 (Absin, Cat # abs131318a), rabbit anti-IFNAR1 (Affinity, Cat # DF6571), anti-Flag M2 Affinity Gel (Sigma-Aldrich, Cat # A2220), and HRP goat anti-mouse IgG (BioLegend, Cat # 405306).

Transfection reagent, LongTrans, was purchased from UcallM (Wuxi, China). Puromycin was purchased from MCE (Monmouth Junction, USA). Actinomycin D (Act D) and protease inhibitor (PI) were purchased from Sigma-Aldrich. Recombinant human IFN- $\alpha$  and IFN- $\beta$  were obtained from PeproTech (Rocky Hill, USA). DRB was purchased from Abcam. Recombinant mouse IFN- $\alpha$  and IFN- $\beta$  were purchased from PBL Assay Science (New Jersey, USA). LEGEND MAX™ Mouse IFN- $\beta$  ELISA Kit (Biolegend, San Diego, USA) was used to measure the concentrations of mouse IFN- $\beta$  in the serum.

### Plasmids

Human RBM47 ORF was amplified from the RNA of 293T cells and then individually subcloned into a eukaryotic expression vector with a FLAG tag or Myc tag. Mouse lenti-shRBM47-GFP-puro plasmid was obtained from iCarTAB (Suzhou, China). Two endonuclease sites (XbaI and FseI) of the pGL3 promoter plasmid (TransVector, Chengdu, China) were used to insert the negative control (NC) and the three RBM47-binding RNA fragments and their mutants. To construct shRBM47, target sequences were inserted into the RNAi-Ready pSIREN-RetroQ-ZsGreen vector. To prepare CRISPR/Cas9 constructs of RBM47, two gRNA sequences individually cloned into LentiCRISPRv2. RBM47 promoter region (-2,000 to +100) were subcloned into the pGL3-basic-Luc vector to analyze RBM47 promoter activity. A DNA-based DENV replicon, DGL2, was generously provided by Dr. Takayuki Hishiki (Kyoto University, Kyoto, Japan) (Kato et al, 2014). The primer sequences are shown in Table EV1.

### Isolation of MEFs, PMs, and BMDMs

Primary MEFs were prepared from IFNAR1<sup>+/+</sup> and IFNAR1<sup>-/-</sup> embryos of day 15 and were cultured in DMEM supplemented with 10% FBS. MEFs were prepared from mouse embryos using standard protocols (Lunde et al, 2007). PMs and BMDMs were prepared as described previously (Bisgaard et al, 2016). Briefly, PMs were isolated from the peritoneal cavity of WT or RBM47<sup>+/-</sup> mice by flushing the peritoneal cavity with 5 ml of ice-cold PBS. Cells were resuspended in RPMI-1640 (Gibco, 12633) media plus 10% FBS and incubated at 37 °C. BMDMs were isolated from female mice by flushing the femur and tibia with PBS. The bone marrow cells were resuspended in RPMI-1640 + 10% FBS + 10% L929-cell conditioned medium and incubated for 7 days at 37 °C and 5% CO<sub>2</sub> with the medium changed every 3–4 days.

### Lentivirus preparation

293T cells were co-transfected with mouse Lenti-shRBM47-GFP-puro (shmRBM47) or control vector (Lenti-U6-shRNA-GFP-puro) and three helper vectors (pGAG, pVSVG, and pREV). After 48 h, the culture supernatant containing lentiviruses was collected. The aliquoted lentiviruses were stored at -80 °C for subsequent experiments. MEF cells were infected with packaged shmRBM47 lentiviruses in the presence of polybrene (Yeasen, Shanghai, China).

### Construction of RBM47<sup>-/-</sup> stable cell lines

293T cells were transfected with two CRISPR/Cas9 constructs of RBM47 (LentiCRISPRv2-RBM47-1 & -2) and selected with puromycin (2  $\mu$ g/ml) for at least 3 weeks. RBM47<sup>-/-</sup> cell lines were obtained by puromycin selection and single-cell clone culture and then verified by western blot analysis.

### Immunoblotting and immunoprecipitation

Cells were harvested in cell lysis buffer containing protease for western blotting and IP. The samples were then centrifuged for 10 min to remove the cellular debris. The lysates were incubated with specific antibodies on a rotor at 4 °C. Protein A/G PLUS-agarose (Santa

Cruz, Dallas, USA) was added to the samples and incubated for an additional 3 h on a rotor at 4°C. After five washes with lysis buffer, the immunoprecipitates were eluted by boiling with loading buffer containing  $\beta$ -mercaptoethanol for 10 min and analyzed using sodium dodecyl sulfate-polyacrylamide gel electrophoresis (SDS-PAGE), followed by transfer to polyvinylidene difluoride (PVDF) membranes. The membranes were then blocked with 5% non-fat milk for 30 min at room temperature and probed with the primary antibodies, followed by HRP-conjugated goat anti-mouse or anti-rabbit secondary antibodies. Immunoreactive bands were visualized using High-SigECL Substrate kits (Tanon, Beijing, China).

### Real-time polymerase chain reaction (PCR)

Total RNA was extracted using the Total RNA Kit I (Omega, Norcross, USA), reverse transcribed using the PrimeScript Master Mix kit (TaKaRa, Kusatsu, Japan), and subjected to real-time PCR analysis to measure mRNA expression levels of the tested genes. The resulting cDNA was mixed with RT-PCR primers and SYBR Premix Ex TaqII and amplified for 40 cycles (95°C for 10 s, 60°C for 10 s, and 72°C for 30 s). The primer sequences used are listed in Table EV1. All qRT-PCR results are represented as relative fold changes after normalization to  $\beta$ -actin controls.

### Dual-luciferase reporter (DLR) assays

50 ng expression plasmid, 50 ng IFN- $\beta$ -Luc/ISRE-Luc, and 5 ng pRL-TK (internal control) were co-transfected into 293T cells plated in 96-well plates. The cells were then infected with virus or stimulated using IFN- $\alpha$  (200 U/ml). Cells were harvested after 24 h, and DLR assays were performed using a luciferase assay kit (Promega, Madison, USA). All reporter assays were performed at least in triplicate, and the results are shown as average value  $\pm$  standard deviation (SD) for each representative experiment.

### Electrophoretic mobility-shift assay

Electrophoretic mobility shift assay (EMSA) was performed according to the standard protocols (Xie *et al*, 2019). The RNA fragments were incubated with purified Flag-tagged RBM47 protein at 37°C for 10 min. Samples were then loaded onto a 6% polyacrylamide mini gel (without SDS) to separate the RNA-protein complexes and free RNAs using electrophoresis (100 V for 1 h) in 0.5 $\times$  TBE buffer on ice. After electrophoresis, RNA fragments were transferred from the polyacrylamide gel to a positively charged nylon membrane (Beyotime, Shanghai, China) in 0.5 $\times$  TBE buffer (380 mA for 1 h) on ice. The nylon membrane was irradiated with 200 mJ/cm<sup>2</sup> of ultraviolet (UV) light at 254 nm in a UV-100 UV crosslinker (Tanon, Beijing, China) with default settings. The nylon membrane was blocked and probed with an anti-biotin antibody for 3 h at room temperature. After washing four times with washing buffer, the blots were incubated with HRP-conjugated secondary antibody and visualized using an ECL kit.

### RNA immunoprecipitation (RIP) assay

293T cells were transfected with RBM47-Flag plasmid. After 2 days, the cells were harvested and subjected to RNA-binding protein

immunoprecipitation (RIP) with an RIP kit using Flag antibody or IgG isotype, according to the manufacturer's instructions (Medical & Biological Laboratories, Nagoya, Japan). The precipitated RNA was reverse transcribed into cDNA and subjected to qRT-PCR analysis. The data are presented as fold enrichment of anti-Flag Ab relative to the IgG group.

### RNA pull-down assay

An RNA pull-down assay was conducted to determine the interaction between RBM47 and IFNAR1 mRNA in 293T cells. Briefly, three RNA segments on the IFNAR1 3'UTR were synthesized and biotinylated by Synbio Technologies (Monmouth Junction, USA). 293T cells transfected with RBM47-Flag were harvested and lysed. The lysates were incubated with 2  $\mu$ g of biotin-labeled RNA for 2 h on a rotor at 4°C. A mixture of Protein A/G PLUS-Agarose and anti-biotin antibodies was added to the samples and incubated on a rotor for an additional 3 h at 4°C. After washing five times, the proteins bound to the beads were subjected to western blotting with a Flag antibody.

### Virus titration

The titers of VSV and HSV-1 in cell-free supernatants were determined with a median tissue culture infective dose (TCID<sub>50</sub>) assay according to standard protocols using Vero cells (Wu *et al*, 2013). Briefly, cells were transfected with different plasmids and then infected with VSV or HSV-1 for 24 h. Culture supernatants containing VSV or HSV-1 viruses were serially diluted with DMEM and then placed on a monolayer of Vero cells in 96-well plates. The virus titer (TCID<sub>50</sub>/ml) was calculated using the Reed-Muench method. One TCID<sub>50</sub>/ml was equivalent to 0.69 pfu/ml (Li *et al*, 2011; Wu *et al*, 2013).

### Viral infection *in vivo*

For *in vivo* viral infection studies, 8-week-old control and mutant mice were infected with VSV ( $1 \times 10^8$  pfu), administered intranasally, or HSV-1 ( $1 \times 10^7$  pfu), injected into the caudal vein. After 24 h, blood was collected from the orbital sinus for the analysis of RNA and viral titers.

### Histological analysis

Lung tissues from control or VSV-infected mice were fixed in 4% formaldehyde solution and embedded in paraffin. Paraffin sections were stained with a hematoxylin-eosin solution, and histological changes were observed using a light microscope (Nikon, Tokyo, Japan).

### Flow cytometry

BMDMs stimulated with IFN- $\alpha$  were analyzed using flow cytometry. Cells ( $1 \times 10^5$  cells/tube) were collected with cold 1 $\times$  PBS and incubated for 30 min at 4°C with FITC-conjugated anti-IFNAR1 (Sino Biological, Beijing, China). After further washing, the cells were analyzed using BD FACS Canto II (Becton, New Jersey, US). FACS data were analyzed using FlowJo software.

## Statistical analysis

Prism 8 software (GraphPad Software, San Diego, USA) was used for the charts and statistical analyses. The data collected were expressed as mean  $\pm$  SD, and the significance of differences between two groups was analyzed using an unpaired two-tailed Student's *t*-test with a cutoff *P* value of 0.05. For multiple comparison expression analysis, all data were normalized to the wild-type controls. For qRT-PCR analysis, the relative expression level of each gene in the control group was set to "1". Significant differences are indicated as follows in all figures: \**P* < 0.05, \*\**P* < 0.01, and \*\*\**P* < 0.001.

## Data availability

This study did not include data deposited in external repositories. All relevant data are available in the manuscript and Supporting Information files.

**Expanded View** for this article is available online.

## Acknowledgements

This work was supported by the Priority Academic Program Development of Jiangsu Higher Education Institutions, Program for Changjiang Scholars and Innovative Research Team in University (PCSIRT), National Natural Science Foundation of China (31770933, 81971917), Natural Science Foundation of Colleges in Jiangsu Province (17KJA310005), Open Project Fund from the State Key Laboratory of Genetic Engineering, Fudan University (SKLGE1903), Postgraduate Research & Practice Innovation Program of Jiangsu Province (KYCX20\_2675), and a grant from Soochow Securities. The funders had no role in the study design, data collection and analysis, decision to publish, or preparation of the manuscript. We would like to thank Drs. Chunsheng Dong, Shaojun Zhang, and Qihan Wu for providing materials and technical assistance.

## Author contributions

KW and JD designed the experiments. KW, CH, TJ, ZC, MX, QZ, and JZ performed the experiments. KW and JD analyzed the data. KW, CH, and JD wrote the manuscript. All authors read and approved the final manuscript.

## Conflict of interest

The authors declare that they have no conflict of interest.

## References

- Antonicka H, Shoubridge EA (2015) Mitochondrial RNA granules are centers for posttranscriptional RNA processing and ribosome biogenesis. *Cell Rep* 10: 920–932
- Bhattacharya S, Katlinski KV, Reichert M, Takano S, Brice A, Zhao B, Yu Q, Zheng H, Carbone CJ, Katlinskaya YV et al (2014) Triggering ubiquitination of IFNAR1 protects tissues from inflammatory injury. *EMBO Mol Med* 6: 384–397
- Bisgaard LS, Mogensen CK, Rosendahl A, Cucak H, Nielsen LB, Rasmussen SE, Pedersen TX (2016) Bone marrow-derived and peritoneal macrophages have different inflammatory response to oxLDL and M1/M2 marker expression - implications for atherosclerosis research. *Sci Rep* 6: 35234
- Blackham S, Baillie A, Al-Hababi F, Remlinger K, You SY, Hamatake R, McGarvey MJ (2010) Gene expression profiling indicates the roles of host oxidative stress, apoptosis, lipid metabolism, and intracellular transport genes in the replication of hepatitis C virus. *J Virol* 84: 5404–5414
- Blanc V, Xie Y, Kennedy S, Riordan JD, Rubin DC, Madison BB, Mills JC, Nadeau JH, Davidson NO (2019) Apobec1 complementation factor (A1CF) and RBM47 interact in tissue-specific regulation of C to U RNA editing in mouse intestine and liver. *RNA* 25: 70–81
- Bock FJ, Todorova TT, Chang P (2015) RNA regulation by poly(ADP-Ribose) polymerases. *Mol Cell* 58: 959–969
- Chateigner-Boutin AL, Small I (2011) Organellar RNA editing. *Wiley Interdiscip Rev RNA* 2: 493–506
- Cieply B, Park JW, Nakauka-Ddamba A, Bebee TW, Guo Y, Shang XQ, Lengner CJ, Xing Y, Carstens RP (2016) Multiphasic and dynamic changes in alternative splicing during induction of pluripotency are coordinated by numerous RNA-binding proteins. *Cell Rep* 15: 247–255
- Dolezal E, Infantino S, Drepper F, Börsig T, Singh A, Wossning T, Fiala GJ, Minguet S, Warscheid B, Tarlinton DM et al (2017) The BTG2-PRMT1 module limits pre-B cell expansion by regulating the CDK4-Cyclin-D3 complex. *Nat Immunol* 18: 911–920
- Fossat N, Radziejewicz T, Jones V, Tourle K, Tam PPL (2016) Conditional restoration and inactivation of Rbm47 reveal its tissue-context requirement for viability and growth. *Genesis* 54: 115–122
- Fossat N, Tourle K, Radziejewicz T, Barratt K, Liebhold D, Studdert JB, Power M, Jones V, Loebl DA, Tam PP (2014) C to U RNA editing mediated by APOBEC1 requires RNA-binding protein RBM47. *EMBO Rep* 15: 903–910
- Gerlach RL, Camp JV, Chu YK, Jonsson CB (2013) Early host responses of seasonal and pandemic influenza A viruses in primary well-differentiated human lung epithelial cells. *PLoS One* 8: e78912
- Gerstberger S, Hafner M, Tuschl T (2014) A census of human RNA-binding proteins. *Nat Rev Genet* 15: 829–845
- Guan R, El-Rass S, Spillane D, Lam S, Wang YD, Wu J, Chen ZC, Wang AA, Jia ZP, Keating A et al (2013) rbm47, a novel RNA binding protein, regulates zebrafish head development. *Dev Dynam* 242: 1395–1404
- He C, Sidoli S, Warneford-Thomson R, Tatomer DC, Wilusz JE, Garcia BA, Bonasio R (2016) High-resolution mapping of RNA-binding regions in the nuclear proteome of embryonic stem cells. *Mol Cell* 64: 416–430
- Hombrink P, Helbig C, Backer RA, Piet B, Oja AE, Stark R, Brassler G, Jongejan A, Jonkers RE, Nota B et al (2016) Programs for the persistence, vigilance and control of human CD8(+) lung-resident memory T cells. *Nat Immunol* 17: 1467–1478
- Kato F, Kobayashi T, Tajima S, Takasaki T, Miura T, Igarashi T, Hishiki T (2014) Development of a novel Dengue-1 virus replicon system expressing secretory Gaussia luciferase for analysis of viral replication and discovery of antiviral drugs. *JPN J Infect Dis* 67: 209–212
- Kim YE, Won M, Lee SG, Park C, Song CH, Kim KK (2019) RBM47-regulated alternative splicing of TJP1 promotes actin stress fiber assembly during epithelial-to-mesenchymal transition. *Oncogene* 38: 6521–6536
- Kong J, Lasko P (2012) Translational control in cellular and developmental processes. *Nat Rev Genet* 13: 383–394
- Li J, Hu DM, Ding XX, Chen Y, Pan YX, Qiu LW, Che XY (2011) Enzyme-linked immunosorbent assay-format tissue culture infectious dose-50 test for titrating dengue virus. *PLoS One* 6: e22553
- Lin X, Wang RF, Zhang J, Sun X, Zou Z, Wang SY, Jin ML (2015) Insights into human astrocyte response to H5N1 infection by microarray analysis. *Viruses-Basel* 7: 2618–2640
- Liu J, HuangFu WC, Kumar KG, Qian J, Casey JP, Hamanaka RB, Grigoriadou C, Aldabe R, Diehl JA, Fuchs SY (2009) Virus-induced unfolded protein

- response attenuates antiviral defenses via phosphorylation-dependent degradation of the type I interferon receptor. *Cell Host Microbe* 5: 72–83
- Lu LF, Zhang C, Zhou XY, Li ZC, Chen DD, Zhou Y, Zhou F, Zhang YA, Li S (2020) Zebrafish RBM47 promotes lysosome-dependent degradation of MAVS to inhibit IFN induction. *J Immunol* 205: 1819–1829
- Lunde BM, Moore C, Varani G (2007) RNA-binding proteins: modular design for efficient function. *Nat Rev Mol Cell Biol* 8: 479–490
- Ma F, Li B, Yu Y, Iyer SS, Sun M, Cheng G (2015) Positive feedback regulation of type I interferon by the interferon-stimulated gene STING. *EMBO Rep* 16: 202–212
- Medioni C, Mowry K, Besse F (2012) Principles and roles of mRNA localization in animal development. *Development* 139: 3263–3276
- Medzhitov R, Janeway Jr C (2000) Innate immunity. *N Engl J Med* 343: 338–344
- Pozzi B, Bragado L, Mammi P, Torti MF, Gaioli N, Gebhard L, García Solá Martín E, Vaz-Drago R, Iglesias Néstor G, García C et al (2020) Dengue virus targets RBM10 deregulating host cell splicing and innate immune response. *Nucleic Acids Res* 48: 6824–6838
- Qian J, Zheng H, Huangfu WC, Liu J, Carbone CJ, Leu NA, Baker DP, Fuchs SY (2011) Pathogen recognition receptor signaling accelerates phosphorylation-dependent degradation of IFNAR1. *PLoS Pathog* 7: e1002065
- Radine C, Peters D, Reese A, Neuwahl J, Budach W, Janicke RU, Sohn D (2020) The RNA-binding protein RBM47 is a novel regulator of cell fate decisions by transcriptionally controlling the p53–p21-axis. *Cell Death Differ* 27: 1274–1285
- Rayon-Estrada V, Harjanto D, Hamilton CE, Berchiche YA, Gantman EC, Sakmar TP, Bulloch K, Gagnidze K, Harroch S, McEwen BS et al (2017) Epitranscriptomic profiling across cell types reveals associations between APOBEC1-mediated RNA editing, gene expression outcomes, and cellular function. *Proc Natl Acad Sci USA* 114: 13296–13301
- Rokavec M, Kaller M, Horst D, Hermeking H (2017) Pan-cancer EMT-signature identifies RBM47 down-regulation during colorectal cancer progression. *Sci Rep* 7: 4687
- Sadler AJ, Williams BRG (2008) Interferon-inducible antiviral effectors. *Nat Rev Immunol* 8: 559–568
- Sakurai T, Isogaya K, Sakai S, Morikawa M, Morishita Y, Ehata S, Miyazono K, Koinuma D (2016) RNA-binding motif protein 47 inhibits Nrf2 activity to suppress tumor growth in lung adenocarcinoma. *Oncogene* 35: 5000–5009
- Salerno F, Paolini NA, Stark R, von Lindern M, Wolkers MC (2017) Distinct PKC-mediated posttranscriptional events set cytokine production kinetics in CD8(+) T cells. *Proc Natl Acad Sci USA* 114: 9677–9682
- Schoenberg DR, Maquat LE (2012) Regulation of cytoplasmic mRNA decay. *Nat Rev Genet* 13: 246–259
- Sutherland LC, Rintala-Maki ND, White RD, Morin CD (2005) RNA binding motif (RBM) proteins: a novel family of apoptosis modulators? *J Cell Biochem* 94: 5–24
- Turner M, Diaz-Munoz MD (2018) RNA-binding proteins control gene expression and cell fate in the immune system. *Nat Immunol* 19: 120–129
- Van Looveren K, Timmermans S, Vanderhaeghen T, Wallaeyts C, Ballegeer M, Souffriau J, Eggermont M, Vandewalle J, Van Wyngene L, De Bosscher K et al (2020) Glucocorticoids limit lipopolysaccharide-induced lethal inflammation by a double control system. *EMBO Rep* 21: e49762
- Vanharanta S, Marney CB, Shu WP, Valiente M, Zou YL, Mele A, Darnell RB, Massague J (2014) Loss of the multifunctional RNA-binding protein RBM47 as a source of selectable metastatic traits in breast cancer. *Elife* 3: e02734
- Wang K, Zou C, Wang X, Huang C, Feng T, Pan W, Wu Q, Wang P, Dai J (2018) Interferon-stimulated TRIM69 interrupts dengue virus replication by ubiquitinating viral nonstructural protein 3. *PLoS Pathog* 14: e1007287
- Wei Y, Zhang F, Zhang Yu, Wang X, Xing C, Guo J, Zhang H, Suo Z, Li Y, Wang J et al (2019) Post-transcriptional regulator Rbm47 elevates IL-10 production and promotes the immunosuppression of B cells. *Cell Mol Immunol* 16: 580–589
- Wu S, He L, Li Y, Wang T, Feng L, Jiang L, Zhang P, Huang X (2013) miR-146a facilitates replication of dengue virus by dampening interferon induction by targeting TRAF6. *J Infect* 67: 329–341
- Xie X, Zou J, Zhang X, Zhou Y, Routh AL, Kang C, Popov VL, Chen X, Wang Q-Y, Dong H et al (2019) Dengue NS2A protein orchestrates virus assembly. *Cell Host Microbe* 26: 606–622.e8
- Yao YX, Yang B, Cao H, Zhao KT, Yuan YF, Chen YS, Zhang ZH, Wang Y, Pei RJ, Chen JZ et al (2018) RBM24 stabilizes hepatitis B virus pregenomic RNA but inhibits core protein translation by targeting the terminal redundancy sequence. *Emerg Microbes Infect* 7: 1–14
- Zhao B-B, Zheng S-J, Gong L-L, Wang Yu, Chen C-F, Jin W-J, Zhang D, Yuan X-H, Guo J, Duan Z-P et al (2013) T lymphocytes from chronic HCV-infected patients are primed for activation-induced apoptosis and express unique pro-apoptotic gene signature. *PLoS One* 8: e77008
- Zheng H, Qian J, Varghese B, Baker DP, Fuchs S (2011) Ligand-stimulated downregulation of the alpha interferon receptor: role of protein kinase D2. *Mol Cell Biol* 31: 710–720